Real-Time Lane Departure Detection Using Google Routes

Nafisa Zarrin Tasnim, Attiq Uz Zaman and M. I. Hayee
Department of Electrical Engineering, University of Minnesota Duluth, Duluth, MN 55812, U.S.A.

Keywords: Lane Departure Detection, Google Routes, Road Reference Heading, GPS Trajectory, Lane Departure Warning System (LDWS).

Abstract: Our previously developed Lane Departure Detection and Warning System (LDWS) used a standard GPS receiver and two algorithms to detect an unintentional lane departure. The first algorithm generated the Road Reference Heading (RRH) from a vehicle's past trajectories, while the second algorithm predicted lane departure in real time using RRH. A significant limitation of this system is the dependency on past trajectories. A vehicle must travel on the road at least once in the past to use that trajectory for RRH generation needed for future lane departure detection. To avoid dependency on past trajectories, this work uses Google routes instead of past trajectories to extract the RRH of any given road. We also compared the RRH generated from a Google route with that of a past trajectory and found both RRHs to be comparable indicating that our LDWS does not need to rely on RRH from past trajectories. To evaluate the accuracy of lane departure detection using Google RRH, we performed many field tests on a freeway. Our field test results show that our LDWS can accurately detect all lane departures on long straight sections of the freeway irrespective of whether the RRH was generated from a Google route or past trajectory.

1 INTRODUCTION

According to the World Health Organization (WHO) report, roughly 1.3 million people die yearly from road traffic crashes (Road Traffic Injuries, n.d.). A survey that examined the national sample of US crashes from 2005 to 2007 identified driver error as the critical reason contributing to 94 percent of crashes (Singh, 2015). Advanced driver assistance systems (ADAS) (Antony & Whenish, 2021) facilitate drivers to make well-informed decisions and consequently help them avoid collisions. The recent advancements in ADAS technologies have increased safety for both drivers and pedestrians. The analysis of a study that estimated the safety benefits of in-vehicle lane departure warning (LDW) and lane-keeping aid (LKA) systems in reducing relevant car injury crashes demonstrated that such systems reduced head-on and single-vehicle injury crashes by 53% at a 95% confidence interval on Swedish roads within a specific speed limit range and road surface conditions (Sternlund et al., 2017). Most Lane Departure Warning Systems (LDWSs) depend on image processing and use cameras, infrared, or laser sensors to estimate a vehicle's lateral shift within a lane to detect an unintentional lane departure (An et al., 2006, Baili et al., 2017, Chen & Boukerche, 2020, Hsiao and Yeh 2006, Jung et al., 2013, Leng & Chen, 2010, Lindner et al., 2009, Yu et al., 2008). Vision-based LDWSs face challenges adapting to diverse weather conditions, handling light changes, and mitigating shadow effects. Blockage of lane markings by other vehicles in LDWS images can also cause detection failures. Real-time processing of captured images is crucial for vision-based LDWS, necessitating synchronous image processing speed to ensure timely and safe detection (Chen et al., 2020). Gamal et al. (2019) also propose a real-time, calibration-free lane departure warning system algorithm utilizing Gaussian pyramid preprocessing and Edge Drawing Lines algorithm, achieving high accuracy (99.36%) and fast processing (80 fps), suitable for integration into self-driving systems in OEM cars, outperforming existing algorithms.

Although advanced image processing techniques work well in diminished lighting scenarios (Dobler et al., 2000, McCall & Trivedi, 2006), many of today's commercially available image processing-based LDWSs have performance issues under unfavorable weather or road conditions like fog, snow, or worn out road markings potentially leading to inaccurate lane detection or overlooking genuine lane markings. To

Tasnim, N., Zaman, A. and Hayee, M.
Real-Time Lane Departure Detection Using Google Routes.
DOI: 10.5220/0012557000003702

In *Proceedings of the 10th International Conference on Vehicle Technology and Intelligent Transport Systems (VEHITS 2024)*, pages 238-248
ISBN: 978-989-758-703-0; ISSN: 2184-495X

tackle the limitations posed by adverse weather conditions and degraded road markings on the performance of image processing-based LDWSs, recent advancements have emerged. For instance, Son et al. (2015) have introduced a lane departure warning system specifically designed to combat illumination challenges prevalent in driving environments. This system demonstrates a 93% detection rate, surpassing traditional approaches, even in scenarios with blurred lane markings or low sun angles. Furthermore, Sang et al. (2024) have developed a self-tuned algorithm that integrates fuzzy logic-based adaptive functions with edge identification and line detection modules. This algorithm aims to enhance image quality in challenging weather conditions, although it may have limitations in handling multiple and curved lines. To address some of these performance issues, Global Positioning System (GPS) technology is integrated within vision-based LDWS. To estimate a vehicle's lateral movement in its lane, such systems employ differential GPS (DGPS) technology (Bajikar et al., 1997) and/or inertial navigation and/or odometry sensors (Toledo-Moreo & Zamora-Izquierdo, 2009) in addition to high-resolution digital maps, making them challenging to deploy and expensive (Clanton et al., 2009). Weon et al. (2021) propose a lane departure detection algorithm for vehicles using Geographic Information System (GIS) and DGPS data with high positioning accuracy under 20 cm. It calculates lane segment distances based on vehicle position, utilizing Bezier curves for curved sections. Although GPS is a very helpful tool for navigation, there are situations in which signal interference, multipath effects, or complex road networks may make it less reliable in streets and urban areas. Rose et al. (2014) demonstrate how combining vision, height measurements, and a lane map can significantly reduce drift when a GPS signal is lost, such as in dense foliage or urban environments. By utilizing existing sensors in commercial vehicles, the system achieves submeter accuracy in lateral distance measurement.

Our previously developed LDWS system was based on a standard GPS receiver without using any image processing or optical scanning devices, or high-resolution digital maps. To detect a lane departure, our developed LDWS system estimated lateral vehicle shift using standard GPS technology. The lateral vehicle shift was estimated by comparing the vehicle trajectory acquired by a standard GPS receiver with a Road Reference Heading (RRH), which was obtained using a newly developed algorithm (Shahnewaz Chowdhury & Hayee, 2021). Our Lane Departure Detection (LDD) algorithm accumulated instantaneous vehicle lateral shifts to detect an unintentional lane departure in real-time (Faizan et al., 2019).

One major limitation of the previously developed LDWS system is the dependency on past trajectories. To detect an unintentional lane departure of any vehicle in real-time on a given road, the vehicle must have traveled on the same road at least once in the past to use that trajectory for RRH generation. During the subsequent trips on the same route, the system can detect a potential lane departure using already generated RRH to warn the driver. To avoid dependency on past trajectories, this work utilizes Google routes from Google Maps instead of past trajectories to extract the RRH of any given road. RRH can be extracted from various GPS navigation systems offered by companies such as Waze, Garmin, TomTom, Sygic, and Apple, among others. However, we opted for Google Maps as it is a widely recognized and popular option. Google routes are available for all roads within the US through Google Maps as navigational routes.We have used the navigational route on any given road provided by Google Maps as a Google route to extract the RRH of that road using our RRH generation algorithm. The extracted RRH from Google routes was used to detect an unintentional lane departure in real-time and alert the driver with an audible warning. We also compared the lane departure detection results using Google RRH to that of the past trajectories and found that lane departure detection resulting from Google RRH and RRH from the past trajectories are comparable. We also performed field tests to evaluate the results showing that our system can accurately detect lane departure on long straight sections of the freeways. This shows the potential of our LDWS to be used for all US roads without the dependency on past trajectories.

The rest of the paper is organized as follows. Section 2 describes the architecture of the system, followed by section 3, which describes RRH generation from Google routes. Section 4 discusses the field tests and results, followed by conclusions in Section 5.

2 SYSTEM ARCHITECTURE

The previously developed LDWS system has been enhanced to work for both past vehicle trajectories and Google routes as shown in Figure 1a. The enhanced LDWS can either generate RRH using past trajectories or from Google routes obtained from

Google Maps. In the updated LDWS, we have incorporated necessary modifications and enhancements of the RRH generation algorithm to accommodate RRH generation from Google routes. With this additional feature of extracting RRH, our LDWS is capable of detecting lane departures of a vehicle in real-time on any road, regardless of whether the vehicle has traveled on that road in the past. Our LDWS compares the vehicle trajectory in real-time with the RRH of that road to detect a lane departure using our LDD algorithm as depicted in Figure 1b where a vehicle trajectory with a lane departure (red dotted line) can be compared with the RRH (blue dotted line) obtained from the Google route (blue solid line) or from one of the past trajectories (not shown in Figure 1b) to determine lane departure using our LDD algorithm (Faizan et al., 2019).

We have also made enhancements to our LDD algorithm to detect lane departure more efficiently. However, this paper is more focused on the details of the new feature of extracting RRH from Google routes obtained from Google Maps. To evaluate the effectiveness of lane departure detection using RRH from Google routes, we have compared the results of lane departure detection using RRH from both Google routes and past trajectories, which will be described in more detail in the field tests and results section.

3 RRH GENERATION FROM GOOGLE ROUTE

We have developed a backend browser-based application where we can specify the start and end points of the desired route on a Google map to obtain the RRH from the Google route on almost any road within the US. The user specifies the start and end location points in the Google map to define the Google route necessary for RRH generation. Our backend browser application accesses Google Maps' API for turn-by-turn directions between the start and

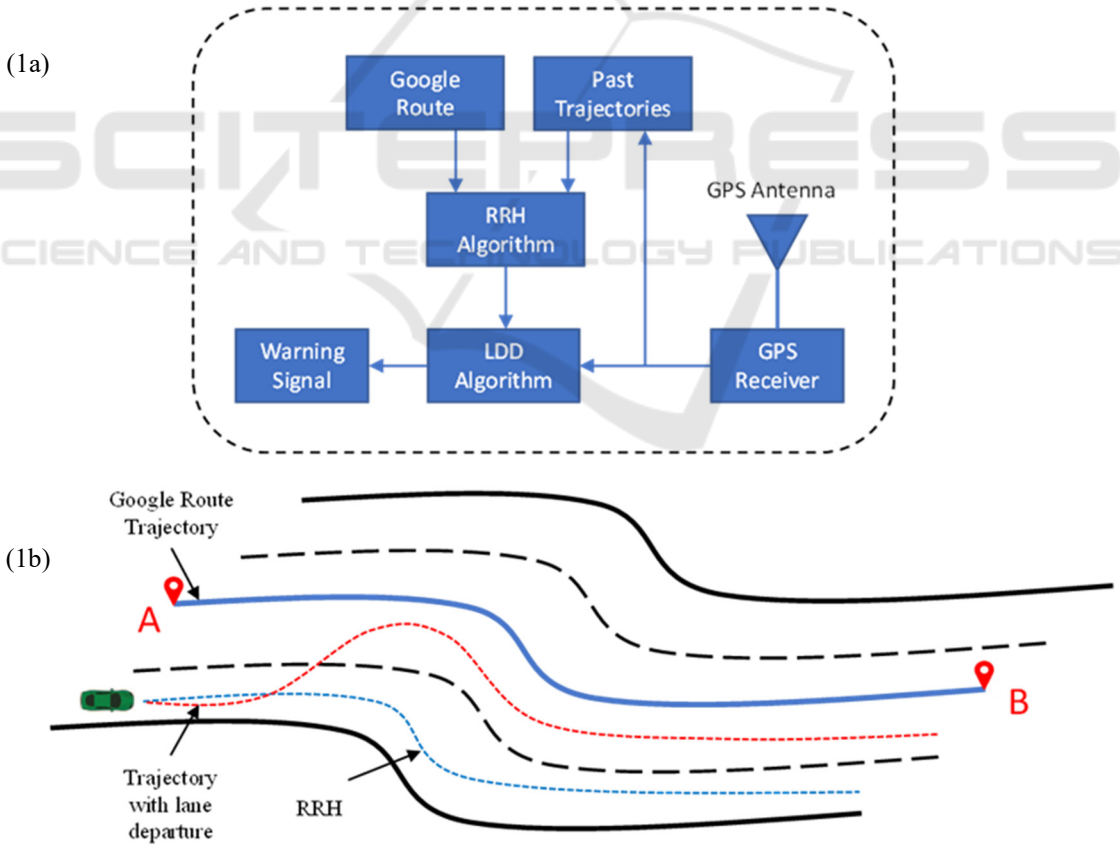

Figure 1: (a) Architecture of the LDWS system. (b) Conceptual diagram demonstrating that RRH (blue dotted line) can be generated from a Google route (blue solid line, where points A and B are the start and end points, respectively) to detect an intentional lane change from right to left (red dotted line). The road illustrated in this figure is a 4-lane road with the Google route shown in the middle.

end points of the route and returns an array of locations with latitudes and longitudes. In this array of locations provided by Google Maps, there are more location points on a curve segment of the road as compared to a straight segment of the road. This array of latitudes and longitudes represents the Google route from which RRH is generated.

We preprocess the array of location points to obtain a uniform distance resolution before applying our RRH generation algorithm. To obtain a uniform distance resolution, we have to access Google Maps API a few times between intermediate location points in the array until we get the desired resolution so that every two consecutive points in the Google Maps array of locations have the same distance as the desired resolution typically in 1 to 3 m range. We have to do more iterations on straight sections in the array as compared to a curve section because there are fewer number of points on a straight section as compared to a curve section.

Our developed RRH generation algorithm characterizes a typical road segment into straight and curve sections, as any typical road can have a combination of straight and curve portions. However, the roads do not curve abruptly; therefore, the section between a straight and a curve is characterized as a transition section by the algorithm. Our algorithm generates an RRH from the pre-processed Google route (uniform array of locations) for any given portion of the road in three major steps.

1) *Identification:* In the first step, all straight, curve and transition sections are identified on that road.

2) *Characterization:* After identification, each section is characterized with a set of optimized parameters that determines the RRH value at any given point on that road. Every straight section is characterized by a Path Average Heading (PAH), as the heading remains constant for the entire length of a straight section. Since the heading of a curve section varies uniformly with distance, it is characterized by a Path Average Heading Slope (PAHS) and an initial heading (IH), where IH is the heading at the

(2a)

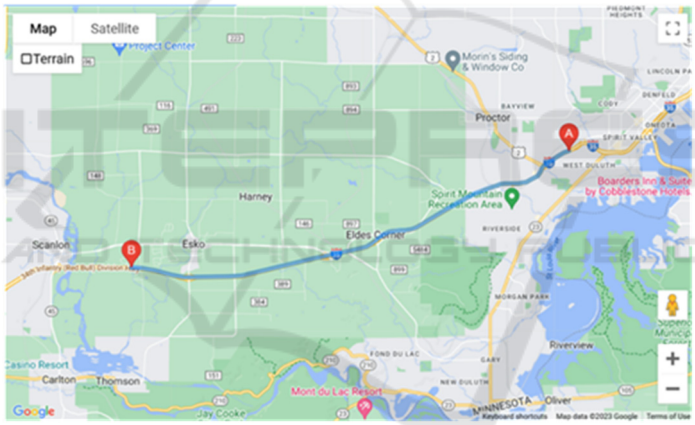

(2b)

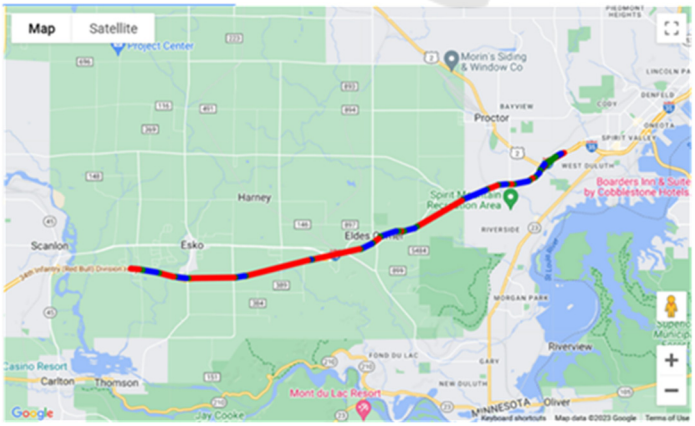

Figure 2: (a) Browser application user interface showing the user-specified route on the Google map to initiate RRH generation from the Google route. Points A and B indicate the start and end location of the desired route, respectively. (b) Google route superimposed on the generated RRH with straight, curve and transition sections indicated by red, blue, and green colors along the route.

beginning point of the curve section. Each transition section is characterized the same way as a curve section.

3) *Aggregation:* Finally, all the individual road sections are combined to obtain a composite RRH for that road to be used with the LDD algorithm for lane departure detection.

The process of generating RRH from the Google route using the browser application is illustrated in Figure 2. Our browser application lets the user specify the start and end points on a given road on Google Maps, as shown in Figure 2a, where points A and B are the start and end points, respectively. After the user specifies the start and end points, our browser application runs our RRH generation algorithm and converts the Google route to RRH consisting of all sections of the road, as shown in Figure 2b, where the red, blue, and green colors along the Google route indicate straight, curve and transition sections, respectively. Our browser application also generates a corresponding datafile containing all the relevant information of all the sections of RRH within the Google route. The information in this datafile contains the start and end points of each section (straight, curve and transition) and the relevant parameter values characterizing each section to determine the RRH value for any point on the road. Using this information, an RRH value can be calculated on any given point of the road between the start and end points specified by the user.

3.1 Algorithm and Parameter Optimization

The implementation steps of our RRH generation algorithm are as follows:

1) First, the Google route is obtained from the browser application containing the array of points in terms of longitude and latitude for each point. The Google route is then pre-processed for uniform distance resolution so that each of the two consecutive points has a constant distance between them (1-3 m range), as explained earlier.
2) Then, the heading between two consecutive points is calculated from the longitude and latitude of those points (Shahnewaz Chowdhury & Hayee, 2021). The heading array is then filtered with a lowpass filter having a corner frequency of 20 Hz (cycles/m) and a total stop frequency of 125 Hz (cycles/m). The filtering is done to smoothen the heading array obtained from Google Maps. The choice of corner and stop frequencies is made to ensure the removal of undesired ripple effects from the heading array.
3) Next, differential headings per meter are calculated from the filtered heading array. The differential heading is then smoothened to further minimize undesired ripples. The smoothening is obtained by averaging differential heading at each point over 40 meters, i.e., ± 20m on either side of the given point.
4) The average differential heading array is then used to identify the straight sections using a threshold of 0.002 deg/m, i.e., any consecutive portion with a differential heading of less than the threshold of 0.002 deg/m will be considered a straight section (Shahnewaz Chowdhury & Hayee, 2021). This step will generate the start and end points of each of the straight sections present in the Google route. Please note that we combined two consecutive straight sections that are not too far apart from each other because a road cannot curve abruptly. For that purpose, we are using a range of 75-100 m as a parameter to combine two consecutive straight sections. Straight sections are then characterized by calculating a PAH between the start and end points of each straight section.
5) After identifying and characterizing straight sections, curve sections are identified and characterized. For this purpose, any portions of the Google route between two consecutive straight sections are considered curve sections, i.e., any contiguous portions on the Google route having a differential heading above the average differential heading threshold of 0.002 deg/m. A PAHS value for each of the curve sections between two consecutive straight sections is then calculated from the average differential heading. The beginning and end points of each of the curve sections are identified where the average differential heading is closest to the calculated PAHS on that curve section. The heading at the beginning point of each curve section becomes the IH for that curve section.
6) The above method of identifying the start and end points of the curve section tends to make the transition sections longer for those curves which have a higher value of PAHS. Therefore, for such curves which have a

PAHS value of >0.02 deg/m, we apply selective thresholding to reduce the lengths of the transition sections and increase the lengths of the adjacent straight sections while keeping the curve section length the same. To achieve this, we increase the threshold of 0.002 deg/m (as in step 4) to 0.01 deg/m (5 times the original threshold) only for those curves which have a PAHS value of >0.02 deg/m.

7) Similarly, some of the curves with a small PAHS may be falsely accounted for as curve sections because their PAHS value is only slightly higher than the threshold (0.002 deg/m) to be identified as curve sections to begin with. To identify and eliminate such false curve sections, the PAHS value for each of the curve sections is recalculated by dividing the difference of the PAH of the two surrounding straight sections by the distance between them. If such a revised PAHS turns out to be smaller than 0.002 deg/m (original threshold), then that curve is absorbed in the surrounding straight sections.
8) The characterized parameters for each straight and curve section are then optimized to minimize the differential heading error (Shahnewaz Chowdhury & Hayee, 2021) between the RRH and Google route heading over the entire portion of each of the straight and curve sections.
9) In the end, transition sections are identified and characterized. Any portion of the Google route between a curve and a straight section is marked as a transition section. The heading at the start point of the transition section becomes the IH of the transition section. The PAHS of the transition section is calculated from the difference in headings between the start and end points of the transition section divided by the distance between them.

To see the effectiveness of the RRH generated from the Google route, we have plotted the Google route heading (green solid line) and the RRH (black solid line) with respect to distance as shown in Figure 3. To identify straight, curve and transition sections on the RRH, a mask with a black dotted line is also shown in Figure 3. The mask has fixed but different heading values for straight, curve and transition sections to distinguish them from each other. The straight sections have a fixed mask value of 252.5º (almost in the middle of Figure 3). For each of the curve and transition sections, two different mask values are attributed to each curve or transition section depending on the PAHS. The mask value for the curve section is either 275º or 230º, depending on whether the PAHS is positive or negative, respectively. Similarly, the mask value for the transition section is 263.75º or 241.25º, depending on whether the PAHS is positive or negative. Please note that specific mask values are chosen to mark the difference between the straight, curve and transition sections within the RRH for the Google route in Figure 3.

The RRH values (black solid line) match pretty well with the Google route heading (green), especially for straight sections (Figure 3). The match between the RRH and the Google route varies for curve sections and we noticed that for one of the sharper curve sections between 1500 m and 2200 m, the match is not as good as for the other portions (Figure 3). This can be improved by tweaking the conditions of the RRH generation algorithm in the

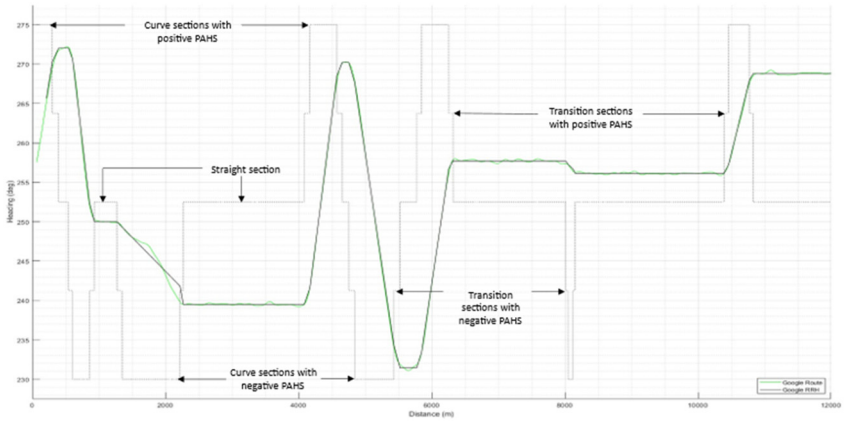

Figure 3: Google route heading (green) and corresponding RRH (solid black) vs. distance. A mask (black dotted line) is drawn to indicate the straight, curve and transition sections.

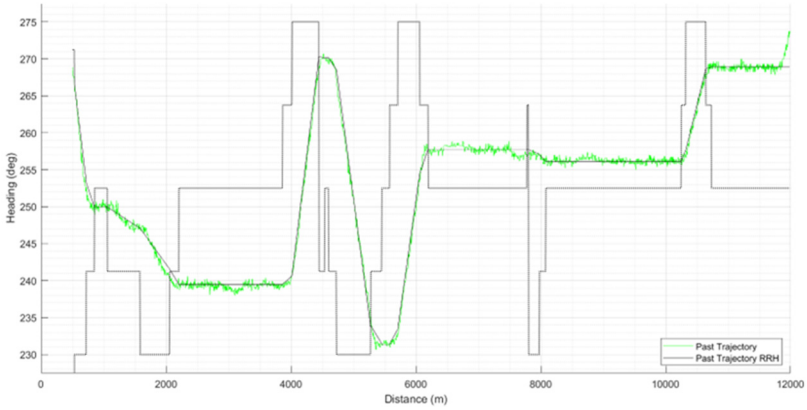

Figure 4: A past trajectory heading (green) and corresponding RRH (solid black) vs. distance. A mask (black dotted line) is drawn to indicate the straight, curve and transition sections.

future. However, our main goal is that the RRH values for the straight sections are reliable so that unintentional lane departure on long stretches of the straight sections can be successfully detected.

We also wanted to compare the accuracy of the Google RRH with the RRH obtained from the past trajectories. Therefore, we applied the modified RRH generation algorithm to one of the past vehicle trajectories obtained on the Interstate I-35 southbound which is the same portion of I-35 for which the Google route was used to extract RRH. The trajectory length was a little shorter than 12 km covering almost the same portion as the Google route in Figure 3. The trajectory heading vs. distance is plotted in Figure 4. For reference, an RRH obtained from this trajectory is also shown in Figure 4. The same mask as in Figure 3 is also used in Figure 4 to differentiate among straight, curve and transition sections of the RRH. Figure 4 shows that the generated RRH (black solid line) follows the vehicle trajectory heading (green) fairly well, indicating that the modified RRH generation algorithm also works well for the past trajectories. In fact, for a much sharper curve present in the trajectory (between 1500 m and 2200 m range), the match between RRH and the past trajectory is much better (Figure 4), as compared to the similar match for the Google route (Figure 3). These discrepancies in Google RRH exist because sometimes the road width changes, i.e., the number of lanes cause abrupt heading deviations in the Google route. However, a more rigorous comparison of the RRH obtained from the Google route and that of the past vehicle trajectory will be made later by detecting lane departures using our LDD algorithm.

4 FIELD TEST AND RESULTS

We performed many field tests to evaluate the RRH obtained from the Google route using our LDD algorithm. All the field tests were performed by driving a test vehicle multiple times on the same 12 km segment of Interstate I-35 southbound, for which an RRH was extracted from the Google route as discussed earlier. Each of the test runs covered a portion of the 12 km road segment to ensure that the test vehicle remained on the same portion of the road for which an RRH was extracted earlier from the Google route. The test vehicle was driven at about the speed limit (70 MPH) on the 4-lane freeway (2 lanes each way) and many lane changes were made intentionally during the field tests. For safety reasons, intentional lane changes were made to test the accuracy of lane departure detection. The vehicle trajectory data for each of the test runs were collected and evaluated with our LDD algorithm to detect the start and end of the lane changes present in each trajectory. Four such trajectories (red, blue, purple & orange colors) from the test runs are shown in Figure 5a, where vehicle heading vs. vehicle traveled distance is plotted. For reference, Google RRH (black solid line) is also shown on the same scale in Figure 5a. In the first two trajectories (red and blue) shown in Figure 5a, a total of 4 lane changes were made, and in the third trajectory (purple), only 2 lane changes were made. There was no lane change made for the fourth trajectory (orange) to ensure that no false alarm was detected by our LDD algorithm. All lane changes were made only on the straight portions of the road as unintentional lane departure is more relevant on longer stretches of straight portions of the road as discussed earlier.

(5a)

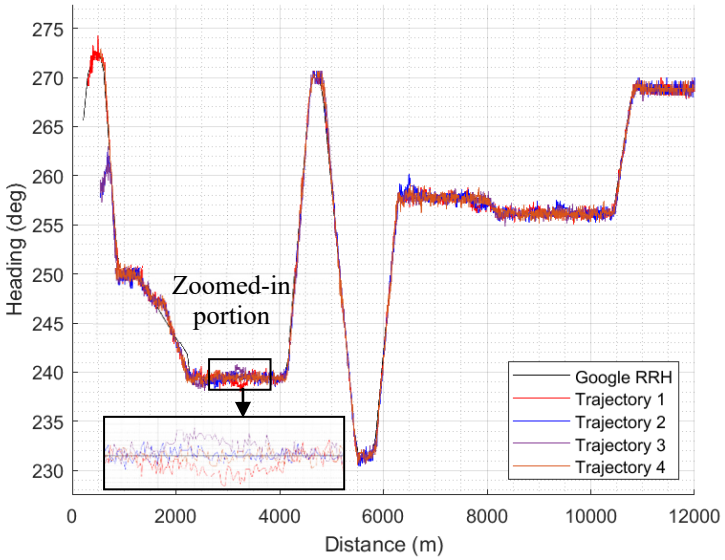

(5b)

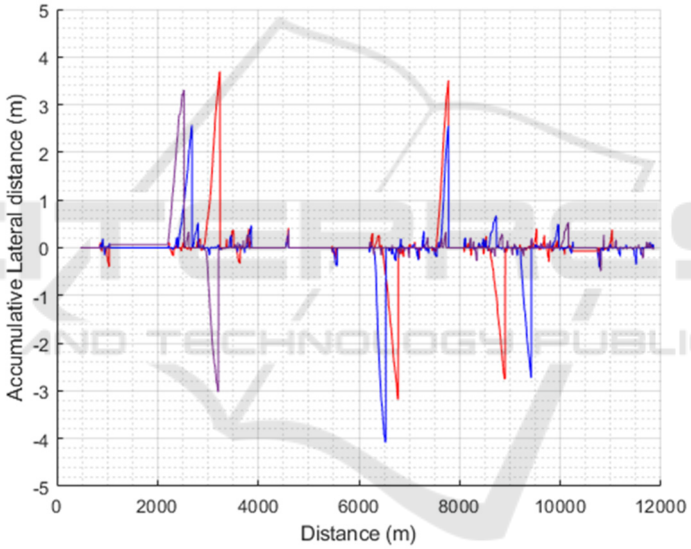

Figure 5: (5a) RRH resulting from the Google route (black) along with the headings of four different trajectories (red, blue, purple & orange) on the same route vs. distance. A zoomed in portion of the Google RRH and 4 trajectories between the 3000 m to 3500 m distance range is shown as an in-set in the figure. (5b) Vehicle accumulative lateral distance vs. traveled distance for four different driven trajectories (red, blue, purple & orange). The vehicle accumulative lateral distance is calculated using Google RRH.

However, from the trajectories shown in Figure 5a, lane changes cannot be visibly identified because there is a very small difference in the heading of a vehicle trajectory and the Google RRH. An example of a lane change is highlighted in a zoomed portion of Figure 5a between the 3000 m and 3500 m range to show that there is a lane change in two of the four trajectories (red and purple) in opposite directions indicated by the vehicle heading deviation in the opposite directions as compared to the Google RRH. Similarly, for the other two trajectories (blue and orange), there was no lane change for this portion, so no noticeable deviation was seen in vehicle heading as compared to the Google RRH.

To evaluate the accuracy of the lane change timing and duration, the accumulative lateral distance of the vehicle for each trajectory vs. traveled distance is shown in Figure 5b. The colors of the accumulated lateral distance for each trajectory are kept the same as in Figure 5a. When the accumulative lateral distance exceeds a certain threshold (~1m) value on either side, it is considered a lane departure. All lane

(6a)

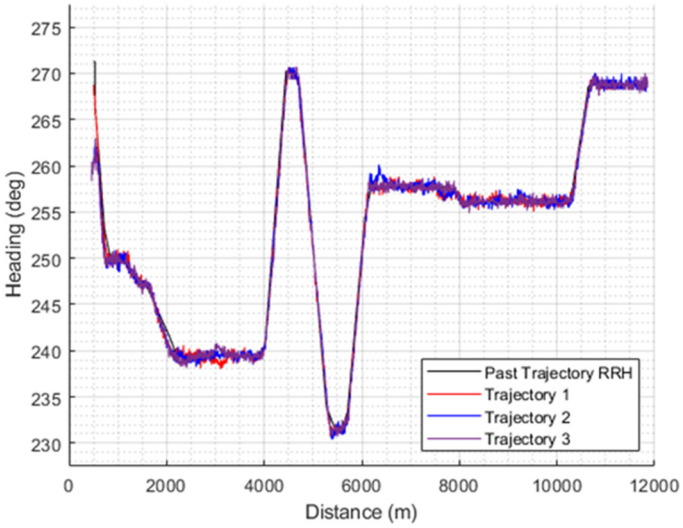

(6b)

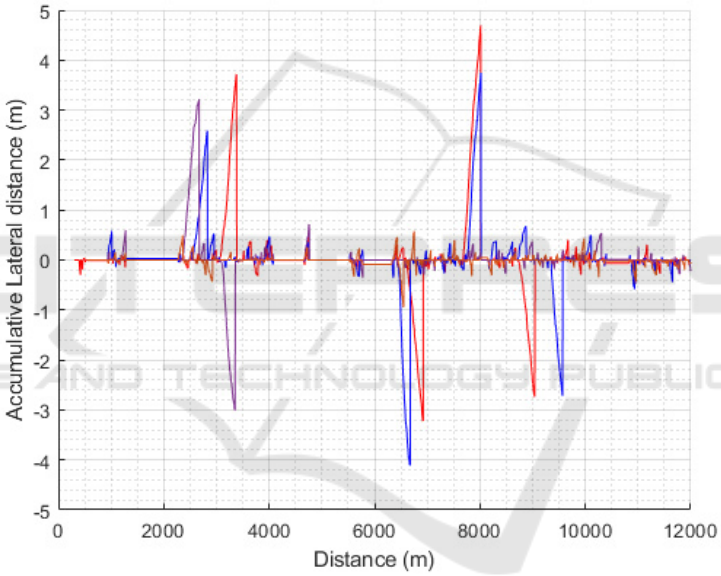

Figure 6: (6a) RRH resulting from one of the past trajectories (black) along with the headings of three different trajectories (red, blue & purple) vs. distance. (6b) Vehicle accumulative lateral distance vs. traveled distance for three different driven trajectories (red, blue & purple). The vehicle accumulative lateral distance is calculated using the RRH extracted from a past trajectory.

changes were accurately identified by our algorithm indicating that the RRH obtained from Google route works well for detecting lane departures, either intentional (lane change) or unintentional. The start and stop of each of the lane changes are clearly identifiable in Figure 5b. For the orange trajectory, where there is no lane change, the accumulative lateral distance never exceeds the threshold of 1 m.

We also wanted to compare the accuracy of lane changes being identified correctly when the RRH was generated from a Google route as well as a past trajectory. We have used Trajectory 4 (orange) of Figure 5 to generate an RRH from it because it does not have any lane changes. The remaining three trajectories (red, blue & purple) from the test runs were used to detect lane changes in them using the RRH extracted from one of the past trajectories (Trajectory 4). The heading of the three trajectories (red, blue and purple) are shown again in Figure 6a, where vehicle heading is plotted with respect to traveled distance. As stated earlier, in two of these three trajectories (red and blue), a total of 4 lane changes were made in each, and in the third trajectory (purple), only 2 lane changes were made. For

reference, RRH extracted from Trajectory 4 has also been shown in Figure 6a.

To evaluate the accuracy of the lane change timing and duration, the accumulative lateral distance of the vehicle for each of the three trajectories using the RRH from Trajectory 4 is calculated and is shown in Figure 6b vs. traveled distance. The colors of the accumulative lateral distance for each trajectory are kept the same as in Figure 6a. All lane changes were accurately identified by our algorithm showing the accuracy of the RRH obtained from a past trajectory using the modified RRH generation algorithm. The start and stop of each of the lane changes are clearly identifiable in Figure 6b. These results indicate that the lane departure can be accurately detected irrespective of whether the RRH is generated from a Google route or a past trajectory for straight portions of the road.

5 CONCLUSIONS

We have successfully developed and implemented the algorithm to extract RRH from a Google route to work with our previously developed LDWS to detect unintentional lane departures. We have evaluated the effectiveness of the RRH from the Google route by performing field tests and comparing the results with that of the RRH from a past trajectory. Our results indicate that our LDWS can accurately detect a lane departure irrespective of whether the RRH is generated from a Google route or a past trajectory for straight portions of the road. However, to ensure accurate lane departure detection on curved road sections, further refinement of the RRH generation algorithm is necessary to align the RRH with the trajectory. Although results have been reported from fourtrips of many along the same 12 km segment of the Interstate I-35 southbound route, it is worth mentioning that this is an ongoing work, and we are in the process of validating this approach with more data from different routes.

ACKNOWLEDGEMENTS

The authors wish to acknowledge those who made this research possible. This work was made possible by Minnesota cities and counties by the Local Road Research Board with support from MnDOT's Office of Research & Innovation.

REFERENCES

An, X., Wu, M., & He, H. (2006). A novel approach to provide lane departure warning using only one forward-looking camera. *International Symposium on Collaborative Technologies and Systems (CTS'06)*, 356–362.

Antony, M. M., & Whenish, R. (2021). Advanced driver assistance systems (ADAS). In *Automotive Embedded Systems: Key Technologies, Innovations, and Applications* (pp. 165–181). Springer

Baili, J., Marzougui, M., Sboui, A., Lahouar, S., Hergli, M., Bose, J. S. C., & Besbes, K. (2017). Lane departure detection using image processing techniques. *2017 2nd International Conference on Anti-Cyber Crimes (ICACC),* 238–241.

Bajikar, S., Gorjestani, A., Simpkins, P., & Donath, M. (1997). Evaluation of in-vehicle GPS-based lane position sensing for preventing road departure. *Proceedings of Conference on Intelligent Transportation Systems*, 397–402.

Chen, W., Wang, W., Wang, K., Li, Z., Li, H., & Liu, S. (2020). Lane departure warning systems and lane line detection methods based on image processing and semantic segmentation: A review. *Journal of Traffic and Transportation Engineering (English Edition)*, *7*(6), 748–774.

Chen, Y., & Boukerche, A. (2020). A novel lane departure warning system for improving road safety. *ICC 2020-2020 IEEE International Conference on Communications (ICC)*, 1–6.

Clanton, J. M., Bevly, D. M., & Hodel, A. S. (2009). A low-cost solution for an integrated multisensor lane departure warning system. *IEEE Transactions on Intelligent Transportation Systems*, *10*(1), 47–59.

Dobler, G., Rothe, S., Betzitza, P., & Hartlieb, M. (2000). *Vehicle with optical scanning device for a lateral road area*. Google Patents.

Faizan, M., Hussain, S., & Hayee, M. I. (2019). Design and development of in-vehicle lane departure warning system using standard global positioning system receiver. *Transportation Research Record, 2673*(8), 648–656.

Gamal, I., Badawy, A., Al-Habal, A. M., Adawy, M. E., Khalil, K. K., El-Moursy, M. A., & Khattab, A. (2019). A robust, real-time and calibration-free lane departure warning system. *Microprocessors and Microsystems*, *71*, 102874.

Hsiao, P.-Y., & Yeh, C.-W. (2006). A portable real-time lane departure warning system based on embedded calculating technique. *2006 IEEE 63rd Vehicular Technology Conference, 6*, 2982–2986.

Jung, H., Min, J., & Kim, J. (2013). An efficient lane detection algorithm for lane departure detection. *2013 IEEE Intelligent Vehicles Symposium (IV)*, 976–981.

Leng, Y.-C., & Chen, C.-L. (2010). Vision-based lane departure detection system in urban traffic scenes. *2010 11th International Conference on Control Automation Robotics & Vision*, 1875–1880.

Lindner, P., Richter, E., Wanielik, G., Takagi, K., & Isogai, A. (2009). Multi-channel lidar processing for lane detection and estimation. *2009 12th International IEEE Conference on Intelligent Transportation Systems*, 1–6.

McCall, J. C., & Trivedi, M. M. (2006). Video-based lane estimation and tracking for driver assistance: Survey, system, and evaluation. *IEEE Transactions on Intelligent Transportation Systems*, *7*(1), 20–37.

Road traffic injuries. (n.d.). Retrieved December 11, 2023, from https://www.who.int/news-room/fact-sheets/detail/road-traffic-injuries

Rose, C., Britt, J., Allen, J., & Bevly, D. (2014). An integrated vehicle navigation system utilizing lane-detection and lateral position estimation systems in difficult environments for GPS. *IEEE Transactions on Intelligent Transportation Systems, 15*(6), 2615–2629.

Sang, I. C., & Norris, W. R. (2024). A Robust Lane Detection Algorithm Adaptable to Challenging Weather Conditions. *IEEE Access*.

Shahnewaz Chowdhury, M. T. H., & Hayee, M. I. (2021). *Generation of Road Reference Heading using GPS Trajectories for Accurate Lane Departure Detection*.

Singh, S. (2015). *Critical reasons for crashes investigated in the national motor vehicle crash causation survey*.

Son, J., Yoo, H., Kim, S., & Sohn, K. (2015). Real-time illumination invariant lane detection for lane departure warning system. *Expert Systems with Applications, 42*(4), 1816-1824.

Sternlund, S., Strandroth, J., Rizzi, M., Lie, A., & Tingvall, C. (2017). The effectiveness of lane departure warning systems—A reduction in real-world passenger car injury crashes. *Traffic Injury Prevention, 18*(2), 225–229.

Toledo-Moreo, R., & Zamora-Izquierdo, M. A. (2009). IMM-based lane-change prediction in highways with low-cost GPS/INS. *IEEE Transactions on Intelligent Transportation Systems, 10*(1), 180–185.

Weon, I. S., Lee. S.G. & Woo, S. H. (2021). Lane Departure Detecting with Classification of Roadway Based on Bezier Curve Fitting Using DGPS/GIS. *Tehnički vjesnik, 28*(1), 248-255.

Yu, B., Zhang, W., & Cai, Y. (2008). A lane departure warning system based on machine vision. *2008 IEEE Pacific-Asia Workshop on Computational Intelligence and Industrial Application, 1*, 197–201.